

1
2
3
4
5
6
7
8
9
10
11
12

The action of octopamine on muscles of *Drosophila melanogaster* larvae.

Short title: octopamine and larval fruit fly muscle

Kiel G Ormerod¹, Julia K Hadden², Lylah D Deady², A Joffre Mercier¹, Jacob L Krans²

¹Department of Biological Sciences, Brock University, Saint Catharine's, Ontario,
Canada

²Department of Neuroscience, Western New England University, Springfield, MA

7 figures

Keywords: neuromuscular junction, force, neuromuscular transduction, biogenic amine

Summary

Octopamine (OA) plays important roles in homeostatic mechanisms, behavior, and modulation of neuromuscular junctions in arthropods. However, direct actions of OA on muscle force production that are distinct from effects at the neuromuscular synapse have not been well studied. We utilize the technical benefits offered by *Drosophila* larvae to distinguish the effects of OA on the neuromuscular synapse from its effects on contractility of muscle cells. We demonstrate that exogenous OA application decreases the input resistance of larval muscle fibers, increases the amplitude of excitatory junction potentials (EJPs), augments contraction force and duration, and at higher concentrations (10^{-5} and 10^{-4} M) affects muscle cells 12 and 13 more than 6 and 7. Similarly, OA also increases the force of synaptically driven contractions in a cell-specific manner. Moreover, this augmentation of contraction force persisted during direct muscle depolarization concurrent with synaptic block by the spider toxin PLTX. OA elicited an even more profound effect on basal tonus. Application of 10^{-5} M OA increased synaptically driven contractions by ~1.1 mN and generated a 28 mN increase in basal tonus when there was no synaptic activation. Augmentation of basal tonus exceeded any physiological stimulation paradigm and can potentially be explained by changes in intramuscular properties. Thus, we provide evidence for independent but complimentary effects of OA on chemical synapses and muscle contractility.

Introduction

The biogenic amine octopamine (OA) is considered to be the invertebrate analog of norepinephrine, and investigations of OA's effects on various arthropod physiological systems have provided insight into fight or flight physiology (Adamo et al., 1995; Hoyle, 1975; Orchard et al 1982; Roeder, 2005). Effects of OA within the CNS have been studied in model arthropod preparations for several decades and have provided insight into important physiological and homeostatic processes, such as energy liberation (Downer, 1979; Fields and Woodring, 1991; Mentel et al., 2003), modulation of metabolic rate, circulation, respiration and ion regulation (Battelle and Kravitz, 1978; Bellah et al., 1984; Blumenthal, 2003; Wierenga and Hollingworth, 1990) and establishment of social hierarchies (Kravitz 1988). Modulatory actions of OA on synaptic potentials at the arthropod neuromuscular junction (NMJ) have been described in great detail (Grundfest and Rueben, 1961; Kravitz et al., 1976; Wheal and Kerkut, 1976; Florey and Rathmayer, 1978; Keshishian et al., 1996; Nagaya et al., 2002). Nevertheless, the actions of OA on muscle force production have not been well investigated in behavioural contexts, and only a few studies have attempted to distinguish intramuscular actions of OA from those at the NMJ (Fisher and Florey, 1983; Fox et al., 2006).

OA was first discovered in the salivary gland of the Octopus, *Octopus vulgaris*, (Erspamer and Boretti, 1951) and has been shown to work through specific receptors (Blenau and Baumann, 2001; Roeder, 1999), often leading to increased intracellular cAMP concentrations (Verlindin et al., 2010). OA acts in several capacities: as a hormone, neuromodulator and transmitter. In addition to its potentiating effect on excitatory junctional potentials (EJPs), OA has been shown to affect a number of behaviours (e.g. locomotion, flight, egg laying, aggressiveness, and ovulation) and is associated with major nervous system functions, such as desensitization and learning and memory (for reviews see, Roeder, 1999; Pflüger and Stevenson, 2005). These alterations in behaviour are accomplished through changes within the CNS as well as changes in the periphery / at muscles. The coordinated interplay between these systems in order to synchronize complex changes in behavioural state requires both neural and neurohormonal mechanisms. OA appears to serve such a coordinating

function by simultaneously altering CNS and peripheral function in response to an altered external environment (fight or flight situation).

Neuromodulators affect many aspects of physiology by acting at multiple levels (e.g. CNS, PNS, muscle; Roeder, 2005). At chemical synapses, the distinction of pre- from post-synaptic actions is traditionally determined electrophysiologically, but often mechanisms downstream of muscle depolarization are presumed complimentary or overlooked (del Castillo and Katz, 1954). Evoked synaptic potentials are often used to interpret presynaptic mechanisms, ideally in conjunction with miniature end plate potentials (mepps). Postsynaptic effects can be easily observed if the modulator induces muscle contractions on its own, as observed for exoskeletal and visceral muscles of cockroach, flies, shrimp, crayfish and others (Adams and O'Shea, 1983; Clark et al., 2008; Meyrand and Marder, 1991; Quigley and Mercier, 1997). It is noteworthy that modulators can act upon a muscle without affecting neuromuscular transduction (Adams et al., 1989). One way to quantify the effect of modulation directly upon the muscle is to employ pharmacological agents to block the presynaptic contribution leaving only the postsynaptic response (Hille, 2001). One may employ calcium channel blockers to inhibit presynaptic calcium influx, but there remain concerns that postsynaptic channels may also be affected. Such concerns are assuaged in model systems wherein one can directly observe the depolarization-force relationship postsynaptically.

Arthropod NMJs have long been used as models to study modulation of chemical synaptic transmission (Bradley et al., 1999) and provide several technical advantages. Arthropod muscles typically have a relatively small number of muscle cells, and in some cases the muscle cells are identifiable (e.g. Hoang and Chiba, 2001; Lnenicka and Melon, 1983; Velez and Wyman, 1978). Muscle cells are typically large, which is favourable for intracellular recordings. In some of these model systems, the motoneurons have also been identified, and the patterns of innervation to specific muscle fibers have been well characterized [cockroach: Ahn and Full, 2002; Zill et al., 1981; fruitfly: Hoang and Chiba, 2001; crayfish: Lnenicka and Melon, 1983; Velez and Wyman, 1978], making it possible to examine modulatory effects on chemical synapses between identified synaptic partners. This also enables one to examine the inherent

ability of modulators to act in a cell-specific manner. Modulatory substances like neurohormones, which interact systemically, need to do so in a coordinated manner, and thus cell-specificity would enable recruitment of selective circuitry. The third-instar larvae of *Drosophila melanogaster* is a model system with both identifiable neurons and muscle fibers (Bradley et al., 1999) facilitating accurate and repeatable experimental recordings (Hoang and Chiba, 2001). *Drosophila* larvae have the added advantage that their neuromuscular synapses contain many modulatory substances (including OA) that have been identified, and the localization of these substances in specific synaptic terminal sub-types is largely mapped (Peron et al, 2009). Moreover, the sequenced *Drosophila* genome and the abundance of mutant and transgenic lines provide tools that promise to fuel a more precise understanding of the cellular machinery and mechanisms underlying synaptic modulation (Bier, 2005).

Here we exploit the technical advantages offered by *Drosophila* larvae to distinguish between modulatory actions of octopamine on chemical synapses from direct effects on contractility of muscle cells. We utilized several strategies to make such a distinction in the location of OA action, investigation of (1) passive membrane properties (i.e. membrane resistance), principal components of (2) excitatory junction potentials, and (3) force production. Furthermore, force augmentation by OA was characterized using the following three assays (a) contraction force when evoked via traditional electrical activation of the motoneuron (i.e. through the synapse), (b) basal muscle tonus in the absence of any synaptic activation, and (c) local depolarization concurrent with synaptic block. We provide evidence that in addition to its ability to augment muscle contractions and potentiate neuromuscular transduction, OA also augments evoked contractions downstream of chemical synapses. The OA-induced changes in basal tonus far exceeded those of evoked contractions and is suggestive of a long-term, intramuscular change by an unidentified factor.

Materials and Methods

1.0 Animals and Basic Preparation

Drosophila melanogaster Canton S (CS) flies, obtained from Bloomington *Drosophila* stock center, were used for all experiments. Flies were reared at 21 °C on a 12:12 light-dark cycle and were provided with either a cornmeal-based medium (Boreal Laboratories Ltd., St. Catharines, Ontario, Canada) including dry yeast, or a Standard Diet (after David, 1962) consisting of 100 g yeast, 100 g glucose, 12 g agar and 10 mL propionic acid (mold inhibitor) combined in 1220 mL H₂O.

Only early wandering stage third instar larvae were selected. Animals were collected from the sides of their culture vials and placed dorsal side up onto a dissecting dish containing either of two hemolymph-like *Drosophila* salines, HL-6 or HL-3.1, the compositions of which have been published (Macleod et al., 2002 and Feng et al., 2004, respectively). All of the experiments outline herein were confirmed in both solutions except contraction recordings (only HL-3.1) and input resistance (only HL-6). A semi-intact larval bodywall preparation (Paterson et al., 2010) was used for recording intracellular electrical signals and force (Fig.1A.i). Briefly, larvae were incised along the longitudinal axis and pinned open. The segmental nerves could be severed near their exit from the ventral ganglion, and the CNS and all other gut organs were removed. The bath was continuously perfused (0.7 mL/min, dish volume ~300 uL) with oxygenated physiological saline, except in the case of application of a toxin (§2.1, below), in which case saline containing the toxin was directly applied and not recirculated in an effort to avoid its residue / remnants confounding future experiments. Experiments followed the same basic application routine: 15 minutes in control saline, application of OA, wash-out for at least twice the duration of exposure to OA. In some experiments, either muscle fibers 12 and 13, or fibers 6 and 7 were lesioned using fine dissection scissors. Unless noted, all muscles were intact.

1.1 Intracellular Recording

Intracellular recordings (Fig. 1A) were obtained using sharp micro-electrodes, produced from thin wall monofilament glass (WPI, Sarasota, FL, USA) using a Flaming-Brown micro-electrode puller (P-97, Sutter Instruments, Novato, CA, USA). Intracellular

recordings were made from longitudinal muscle fibers 6, 7, 12 and 13 across abdominal segments 3, 4 and 5. The anatomy and position of longitudinal muscles (see Fig. 1A) in these centralized segments are highly conserved and function to shorten body length during rhythmic contractions of locomotion. Intracellular data from homologous muscle fibers (i.e. m. 6 and m. 7; m. 12 and 13) were combined and are reported as such. Synaptic potentials were elicited by stimulating all segmental motoneurons via a glass suction electrode and using a Grass S88 stimulator and stimulus isolation unit (Grass Technologies, West Warwick, RI, USA). Single impulses were generated at 0.2 Hz, 0.5 ms pulse duration and ~115% of the voltage needed to attain maximal compound EJP amplitude. Stimulus frequency and voltage are described in text for contraction recordings as some experiments utilized direct stimulation of the muscle (§2.1, below).

EJPs were recorded using either an AxoClamp 2B (Molecular Devices, Sunnyvale, CA, USA) or Neurodata IR283A (Cygnus Technology, Delaware Water Gap, PA, USA) intracellular recording amplifier. Three principal components were measured from these recordings: (a) maximum amplitude (b) rise time constant (τ_{rise} : latency to reach ~63% of peak), and (c) decay time constant (τ_{decay} : latency to decay 63% from peak). Current injection was required for input resistance measurements and accomplished using the single-electrode voltage / current clamp technique.

2.0 Contractions

2.1 Synaptically Evoked Force

A force transducer was custom-designed and constructed using high gage factor silicon wafer strain gages (Micron Instruments, Simi Valley, CA, USA) and was utilized in all experiments recording evoked contractions (Fig. 1A.iii; after Paterson et al., 2010). Briefly, custom designed silicon wafers were placed in a double Wheatstone Bridge configuration around the weakest point of a 0.02" polycarbonate beam (1.5 cm x 5 cm), yielding a signal:noise limited resolution of ~600 nN. As with any force sensing device, the modulus of strain of the beam must be matched to the force generated. This newest generation of force beam in our laboratory was designed with whole body *Drosophila melanogaster* contractions in mind and provides favorable resolution

(amount of silicon deformation) and stiffness (approach to isometric conditions) given available fabrication materials.

Muscle fiber length was controlled using the following procedure (except during basal tonus recordings). Prior to acquiring experimental data, evoked contractions were monitored as muscle length was sequentially increased until reaching the peak of the length–tension curve. This peak was identified empirically as the muscle length just shorter than the length at which a decrease in force occurred. This method was utilized as one part of working toward the isometric condition. Additionally, video was acquired through the microscope (TCA 5.0 MP, 8 fps, Ample Scientific, Norcross, GA, USA) while adjusting the muscle length. Length change during contraction was measured as the difference between the animal's length prior to and after contraction (analysis performed with Image J, NIH, Bethesda, MD, USA). Force data were rejected if Δ animal length exceeded 5% (~200 μm of a 4 mm larvae; mean of 10 randomly selected videos was $3.62 \pm 0.49 \%$). However, given that much of the bodywall tissue of these larvae can be modeled as a viscous material, small changes in total animal length cannot ensure that a particular segment's muscle fiber length does not change relative to the length of fibers in abutting segments.

Stimuli were delivered to segmental nerves through a glass suction electrode or directly to the muscles to evoke contraction. Stimulus duration was 700 μs during experiments measuring contractions, but reduced to 400 μs during V_m recordings. Duration was also reduced during direct muscle activation, and stimuli were delivered directly through the saline approximately two mm from the longitudinal muscles. Voltage was decreased an order of magnitude below that required for neuronal activation and then was increased progressively until contraction amplitude matched that of synaptically evoked contractions prior to changing to direct stimulation. In these latter experiments, a spider toxin (ω -plectoxin-Pt1a: PLTX-II, Alamone Labs, Jerusalem, Israel) was applied to block synaptic transmission. PLTX-II is a 44 amino acid peptidyl toxin produced by *Plectreurys tristis* and is known to effectively block voltage-gated, pre-synaptic calcium channels (Braton et al. 1987, Leung et al., 1989).

It has been well documented that the larval *D. melanogaster* preparation exhibits decay in several physiological properties (Macleod et al., 2002, Stewart et al., 1994).

Extensive work has been done to maximize preparation longevity using hemolymph-like saline (Stewart, 1994, Krans et al., 2010). Moreover, scaling equations are routinely used to account for the progressively depolarized membrane potentials that often occur over time in larval bodywall muscle (Martin, 1976; Stevens, 1976; McLachlan and Martin, 1981). A descriptive model of decay in contraction force is necessary to quantify the change in force production at various times post-dissection. Although a given contraction may be lower than initial peak values obtained immediately post-dissection, it may actually correspond to an augmentation given the normal decay in contractile physiology. We quantified this physiologic 'run-down' in peak force over two hours of recording (Fig. 2). Decay in peak force evoked by equal trains of nerve stimulation - wherein no change in saline composition was administered - were better fit by an exponential decay function than a linear function (Fig. 2B and 2C; $R^2 = 0.95$ and 0.72 , respectively; $P < 0.01$, both using *Pearson's Correlation*, $n=10$). In a minority of cases, a logarithmic fit (e.g. $F_{pk} = -0.155 \ln(t) + 1$; not shown) was also an acceptable model; i.e. two of these 10 experiments dedicated to quantifying decay were marginally better fit with a logarithmic function than an exponential function. Based on historical models of contraction run-down and a closer examination of residuals (Fig. 2C; the difference between observed data and fitting models), we chose to use an exponential fit. We evaluated 103 additional preparations for which some manipulation of the preparation saline was made but full reversal was attained, and in 87 of those 103 preparations (84%), $R^2 > 0.92$ using an exponential fit.

2.2 Basal Tonus:

The posterior end of each dissected third-instar larva was pinned-down to a custom-made recording dish. The anterior of the larva was attached to a Grass FT03 tension transducer (Grass Instruments, Quincy, MA, USA) using a custom metal rod with a bent minuten pin at the distal end. The minuten pin was inserted into the larva in a manner which ensured muscle movements were parallel to the motion of the transducer spring. Care was taken to ensure that the preparation was not overstretched. To maximize the force of contraction, the larva was raised slightly off the dish to prevent friction. Contractions were amplified using a MOD CP122A amplifier (Grass

Technologies, W. Warwick, RI, USA). The signal was digitized using a DATAQ DI-158U data acquisition device, then viewed and analyzed using DATAQ acquisition software. Solutions were applied directly to the larvae using a peristaltic pump (0.7 mL/min, volume of dish ~300 μ L). Excess solution was removed using continuous suction. Baseline recordings were taken for at least 5 minutes prior to exchanging saline for experimental solutions.

3.0 Data Analysis

EJPs were averaged into 30 second time intervals (six EJPs per interval) over each 15 minute trial, and each time point was then averaged over the replicate trials for each condition. Likewise, 8- 10 contractions were averaged every five minutes (using a 35 or 45 s inter-trial pause), and contraction trials typically lasted about two hours. Thus, hundreds of total repetitions for each experimental condition were used in computing averages. However, the number of replicates (n) reported indicates the number of animals, not repetitions. Standard error of the mean is computed using the number of animals and is reported unless otherwise noted. Fit equations, correlation and Pearson's values, and t-Test probabilities were generated using the statistics toolbox in MATLAB (Mathworks, Natick, MA, USA). Sigmaplot (Systat Software, San Jose, CA, USA) was used to generate logistic equations (three parameters plus intercept) and ANOVAs. Formulae are given in figure legends where possible, whereas statistical findings are reported in text.

Some data have been reported previously in abstract form (Ormerod et al., 2012).

Results:

We first characterized the [OA]-dependency of EJP principal components (change in peak EJP amplitude, and rise and decay times: τ_{rise} and τ_{decay} , respectively) when evoked via neural stimulation. At bath concentrations of greater than 10^{-7} M, OA augmented EJP amplitude significantly (Fig. 3; $P < 0.01$), and the effect was reversible. At 10^{-4} M, OA's effect on EJP amplitude required approximately two times the exposure duration for complete reversal and washout (Fig. 3B), but at all lower concentrations tested, EJP amplitude returned to control values in less than 5 min of washing in control saline (perfusion rate = 0.7 mL/min). At 10^{-5} and 10^{-4} M [OA], the augmentation of EJP amplitude was significantly greater in muscles 12 and 13 than in muscles 6 and 7 ($P < 0.01$, Fig. 3C). Specifically, the mean augmentation of EJP amplitude in muscles 6 and 7 at the two highest concentrations of OA was 29.89% of control amplitude, whereas the mean augmentation of EJP amplitude in muscles 12 and 13 was 39.99%. Both rise and decay time constants increased with OA-dependent augmentation of EJP amplitude (Fig. 3D). Evaluating these changes relative to controls, τ_{rise} increased ~15% per molarity order of magnitude ($\% \Delta \tau_{\text{rise}} = 0.15 * \log [\text{OA}] (\text{M}) + 1.15$, $R^2 = 0.93$) whereas τ_{decay} increased 6.65% per molarity order of magnitude ($\% \Delta \tau_{\text{decay}} = 0.067 * \log [\text{OA}] (\text{M}) + 0.562$, $R^2 = 0.84$). We next attempted to ascertain if the OA-mediated effects on EJP amplitude were occurring in part through non-selective activation of tyramine receptors. We co-applied 10^{-4} M [OA] and a tyramine receptor antagonist, yohimbine (10^{-5} M), and observed a $24.2 \pm 1.15\%$ increase in EJP amplitude, which was not significantly different ($P = 0.095$) from application of 10^{-4} [OA] alone ($28.83 \pm 1.79\%$).

To characterize the action of octopamine on the muscle membrane, we measured voltage deflections to brief (< 1 s) pulses of hyperpolarizing current steps (Fig. 4A: 4, 6, 8, 10, and 12 pA) to estimate input resistance of the muscle cells. At concentrations greater than 10^{-5} M, OA significantly decreased input resistance (Fig. 4B) and did so in a dose-dependent manner (Fig. 4C, $P < 0.01$ for 10^{-5} through 10^{-3} M [OA]).

Octopamine modulated several components of contraction force. Most notably, at even low doses, octopamine increased the peak amplitude of contractions elicited by stimulating the motor nerve at 25 Hz (Fig. 5A). Modulation of contraction force was significantly dependent upon changes in [OA] (Fig 5B, one way non-parametric analysis

of variance, $P < 0.01$). The OA-dependent augmentation of force saturated above 10^{-4} M [OA] and yielded $32.3 \pm 6.72\%$ greater force than observed in controls (black squares Fig. 5B). When combined with the tyramine receptor antagonist, yohimbine (10^{-5} M), [OA] at 10^{-4} M augmented force $29.34 \pm 2.26\%$, which was not statistically different from OA alone ($P < 0.05$). There was a minimal level of augmentation observed at concentrations of 10^{-8} - 10^{-7} M [OA] (Fig. 5B: $11.26 \pm 7.38\%$; $n=11$ animals). The dose at which 50% of OA augmentation was achieved was estimated using a standard logistic equation and was 5.3×10^{-6} M [OA].

Since high doses of octopamine induced a greater change in EJP amplitude among muscles 12 and 13 than muscles 6 and 7, we evaluated the cell-specificity of its action upon contraction force by ablating either muscles 6 and 7 or muscles 12 and 13. Greater augmentation was observed when muscles 12 and 13 were left intact than when muscles 6 and 7 were left intact (Fig. 5B). Across all doses tested, augmentation of force in muscles 12 and 13 was $28.59 \pm 1.88\%$ greater than in muscles 6 and 7. The augmentation of force in muscles 12 and 13 was significantly greater than the value obtained with all fibers intact at 10^{-4} and 10^{-3} M [OA] ($6.04 \pm 0.88\%$, $P < 0.01$). Likewise, the augmentation of force observed at these concentrations in muscles 6 and 7 was significantly lower than that observed when all fibers were intact ($-4.51 \pm 0.64\%$, $P = 0.0094$). The greater modulation of contraction in muscles 12 and 13 compared to 6 and 7 corresponds well with the effects of OA on EJP amplitude recorded from these two pairs of muscles (Fig. 3D).

We hypothesized that the OA-induced augmentation of contraction force would shift the motoneuron frequency – force relationship to the left, yielding greater forces in octopamine than control saline from otherwise equivalent motoneuron trains. We tested this hypothesis by selecting a single concentration of octopamine (5.5×10^{-6} M, nearly equivalent to the EC_{50} indicated above) and measuring force of contraction prior to, during, and after OA application. OA decreased the frequency required to generate 90% of the maximal force, decreasing it nearly in half, from 23.01 Hz in control saline to 12.75 Hz in OA-containing saline (Fig. 5C). Likewise, there was a shift in the frequency required of the motoneuron to yield 50% of tetanic force from 10 Hz in control saline, to 6.9 Hz in OA-containing saline (Fig. 5C).

Octopamine also increased the duration of contractions, both by decreasing rise time and increasing decay time. At the highest concentration of OA examined, 10^{-3} M, the force associated with evoked contractions occasionally required more than 2 s to decay after synaptic activation, yielding a very large and variable increase in mean decay time (101.7 ± 62.68 ms; $76.45 \pm 47.12\%$ increase; Fig. 5D). The OA-dependent increase in decay times persisted in a dose-dependent manner across all doses examined, and was statistically significant at concentrations greater than 10^{-5} M [OA] ($P=0.049$ at 10^{-5} M, $P \leq 0.011$ at higher [OA]). Likewise, though of opposite sign, rise time of contraction progressively decreased with [OA] (Fig. 5D; $P=0.052$ at 10^{-5} M, $P<0.01$ at higher [OA]).

We next evaluated changes in basal tonus as an indication of extra-synaptic action of octopaminergic modulation. In the majority of experiments OA was bath applied to preparations used exclusively for basal tonus (Fig. 1B) that eliminated synaptic discharge. In a few experiments, suction stimulation of severed segmental nerves was utilized (Fig. 1A) to provide simultaneous comparison of augmentation to basal tonus with augmentation of synaptically driven contractions. For example, application of 10^{-5} M [OA] induced a large, slow contraction that reached a stable level after about three minutes (Fig. 6A). This same concentration of OA yielded a 21.4% increase in contraction force evoked by stimulation of the segmental nerve at 25 Hz for 1 s (Fig. 6A, insets at far left and right). This latter effect corresponded to ~ 1.1 mN and was *many* times smaller than the slow, progressive increase in basal tonus, which was 28 mN (Fig. 6A). Basal tonus increased with [OA] in a dose-dependent manner (Fig. 6B). To evaluate the magnitude of augmentation and compare it to that observed upon synaptic activation, we fit the change in basal tonus with a simple logistic equation (Fig. 6C; total force, sufficiently consistent across animals;). The concentration of [OA] at which 50% of the total augmentation in basal tonus was observed (i.e. 6.65 mN; Fig. 6C), was determined to be 8.8×10^{-7} M, whereas 90% of maximal augmentation (11.95 mN) was attained in 1.4×10^{-5} M [OA].

Given this indication that a profound post-synaptic action of OA may exist *independently* of synaptic activation, we next examined forces driven by direct depolarization. These experiments utilized the spider toxin PLTX-II, which is a known

pre-synaptic voltage-gated calcium channel blocker (Branton et al., 1987). Early work characterizing the action of the PLTX toxin did not use multiple stimuli as we are accustomed to in driving contractions. We therefore recorded the persistent failure of the synapse in two series of experiments (Fig. 7). Axonal stimulation of the motoneuron in the presence of 10^{-8} M [PLTX-II] yielded persistent decay in the amplitude of contraction force and a complete abolition of force within 30 minutes (Fig. 7A). The persistent loss of contraction during axonal stimulation corresponded to a loss of synaptic depolarization of the muscle (Fig. 7B). However, contractions were recovered with direct depolarization by ejecting the axons from the glass stimulating electrode, moving the electrode 2 mm further from the NMJ and increasing the stimulus intensity slightly (Fig. 7C). Contraction amplitude and rise slopes were not statistically different between synaptic and direct stimulation of the muscle ($F_{pk-syn} = 3.21$ mN vs. $F_{pk-direct} = 3.26$ mN; $t_{rise-syn} = 1.066$ s vs. $t_{rise-direct} = 1.073$ s; $P > 0.05$, $n = 8-10$ each pair). Contraction decay times were substantially longer and more variable in saline containing PLTX and OA than in controls (data not shown). Octopaminergic augmentation of contractions was maintained in the absence of synaptic depolarization, though at a consistently lower magnitude (Fig. 7D). Indeed, there was no significant difference in the rise slope of logistic functions used to fit these two data sets – either with or without synaptic activation (Fig. 7D; peak rise in force per log M [OA] = 9.5%, peak rise in force per log M [OA]+PLTX = 8.7%, $P > 0.05$). Specifically, the concentration of OA at which 50% of the maximal effect was observed was between 10^{-5} and 10^{-6} M in both cases (9.3×10^{-6} M [OA] in PLTX-containing saline vs. 5.3×10^{-6} M [OA] in control saline), and 90% of the effect was obtained between 10^{-4} and 10^{-5} M [OA] in both conditions (8.0×10^{-5} M [OA] in PLTX-containing saline vs. 3.8×10^{-5} M [OA] in control saline).

Discussion

We have demonstrated that octopamine elicits distinct but complimentary actions on muscle cells and on neuromuscular synapses. EJP amplitudes increased by ~35% (all muscles, 10^{-4} and 10^{-5} M [OA]), and the force associated with synaptically driven contractions increased similarly, ~32%. OA also augmented force significantly in directly stimulated muscles after blocking neuromuscular synapses. The significant OA-induced reduction in input resistance and dramatic increases in muscle tonus, far exceeding synaptically driven changes in force-production, provide additional evidence for an independent postsynaptic action of OA. Additionally, OA was found to consistently potentiate EJPs in some fibers to a greater extent than others, thereby providing evidence for cell-specificity. OA also significantly shifted the motoneuron frequency – force relationship to the left; 90% of maximum force was obtained in 5.5×10^{-6} M [OA] at only 55% of the stimulus frequency required in control saline. The greatly increased relaxation / decay time of contractions, taken together with augmented force, suggests a robust action upon muscle contractile properties and work potential.

Octopamine elicited a dose-dependent decrease in muscle fiber input resistance, suggesting that OA opens ion channels and/or greatly activates exchanger rates at the muscle membrane (Fritz et al., 1979; Walther and Zittlau, 1998). Given the significant reduction in input resistance, Ohm's law predicts a concurrent reduction in EJP amplitude. However, application of OA demonstrated a substantial dose-dependent *increase* in EJP amplitude relative to control preparations, suggesting that the drop in input resistance is more than compensated by an increase in synaptic current. It has been shown previously that octopamine increases mepp frequency (Evans, 1981; O'Gara and Drewes, 1990), but previous reports do *not* indicate an effect of OA on mepp amplitude (Evans, 1981). Nonetheless, we observed a significant decrease in muscle membrane resistance ($\leq 20\%$) *and* an increase in post-synaptic potential amplitude. A plausible explanation is that OA increases EJP amplitude by increasing the amount of transmitter released per nerve impulse. Hidoh and Fukami (1987) reported that OA increased EJP amplitude in mealworm larvae (*Tenebrio molitor*) by roughly 40% at concentrations at or above 10^{-6} M. They also observed a significant increase in mepp frequency and no change in mepp amplitude following OA application

(Hidoh and Fukami, 1987). These observations, coupled with a significant increase in quantal content, led them to speculate an increase in intracellular Ca^{2+} was responsible for the increased EJP amplitude. More recently, OA has been shown to enhance transmitter release in *Aplysia* neurons via an increase in calcium entry at synaptic boutons (Jin et al., 2012).

Of the principle parameters of contraction force altered by OA, the most noticeable *initially* was a significant increase in synaptically driven force-generation. Concentrations above 10^{-4} M [OA] generated ~32% greater force than observed in control saline, which was comparable to the observed increases in EJP amplitude (~35%) at the same OA concentration. OA has previously been demonstrated to have an effect on twitch amplitude in a variety of arthropod species (cricket: O’Gara and Dewes, 1990; locust: Evans 1981). OA has also been shown to potentiate striated muscle contractions in crayfish (Fisher and Florey, 1983), lobster (Kravitz et al., 1980) and crab (Rane et al., 1984). The EC_{50} for force augmentation reported here (5.3×10^{-6} M) is similar to what Evans (1981) reported for the effect of OA on twitch amplitude in locust (3.3×10^{-6} M). OA application also significantly increased the decay time constant in the present study, which is consistent with previous reports investigating cricket and locust muscles (O’Gara and Dewes, 1990, O’shea and Evans, 1979, Klassen and Kammer, 1985, Whim and Evans, 1988, 1989). Here again the effects observed on EJPs translated well to force recordings; the decay time constant for EJP was 22% greater than control (10^{-5} M [OA]) and the decay time constant for synaptically driven contraction force at the same concentration was 30% greater than control.

Although the OA-dependent changes in contraction force during synaptically driven recordings were significant, they were small in comparison to the effects of OA on basal tonus. Application of 10^{-5} M [OA]-containing saline resulted in a 1.1 mN increase in the force generated by synaptic activation, compared to a 28 mN change in basal tonus without synaptic activation. Not only do these results highlight a profound postsynaptic effect, but the 28 mN of basal tonus augmentation is drastically larger than what has been observed under normal physiological stimulation paradigms (Paterson et al., 2010). This provides additional evidence that OA may be working on extrajunctional receptors or influencing other intramuscular properties (discussed below). To verify that

the effects on basal tonus were independent of the synapse, we pharmacologically blocked the presynaptic contribution and directly depolarized muscles. Under these conditions, ~22% of the OA-dependent force generation persisted (at 10^{-4} and 10^{-3} M), suggesting that only about one-third of the 32% augmentation of force via synaptic activation is attributable to larger EJPs. This observation provides further evidence for an independent postsynaptic target of OA. Moreover, these results demonstrate that in the presence of a modulatory substance, the EJP is not necessarily the sole indicator of force production, which suggests that caution should be taken in drawing conclusions about muscular force from electrophysiological data from the neuromuscular synapse.

In addition to the dose-dependent increases in EJP amplitude following OA application, OA potentiated EJPs more strongly in some muscle fibers (12 and 13) than in others (6 and 7). Monastirioti et al. (1995) demonstrated differential OA expression within motoneuron subtypes innervating *Drosophila* larval body wall muscles using immunoreactivity. They concluded that OA-immunoreactive boutons innervated muscles 12 and 13, but not 6 and 7. If the presence of OA-immunoreactivity is tightly correlated with the capacity to be modulated by exogenous OA, we would have predicted little or no increase in EJP amplitude for fibers 6 and 7. Thus, the presence or absence of OA within synaptic boutons does not correlate well with the ability of the innervated muscle fibers to respond to exogenous OA application. This conclusion is consistent with the accepted view that OA acts as a neurohormone (e.g. during fight or flight) in addition to its function as a neurotransmitter. Our data indicate that the absence of OA-immunoreactivity in muscles 6 and 7 does not exclude them from modulation by OA, but may indicate the presence of additional cellular machinery (i.e. receptors) in muscles 12 and 13 since that pair exhibited greater augmentation of EJP amplitude and decay time.

Our data support that OA can and does act in a cell-specific manner in muscles. We thus sought to determine whether this cell-specific difference in EJP potentiation extended to force generation. Using an ablation technique, we eliminated muscles 6 and 7 from our recordings and examined OA-dependent force changes associated with synaptically driven contractions. With only muscles 12 and 13 intact, at 10^{-4} and 10^{-3} M [OA] we observed a $38 \pm 5\%$ increase in force, a $6.0 \pm 0.9\%$ increase over the augmentation observed with all muscles intact. Next, we eliminated muscles 12 and 13,

leaving 6 and 7 intact, and observed a $28 \pm 2\%$ augmentation in force at 10^{-4} and 10^{-3} M [OA], a $4.5 \pm 0.6\%$ decrease compared to all fibers intact. These results demonstrate that the cell-specific effects upon EJPs correspond to complementary cell-specificity in force augmentation.

It has been shown for a multitude of neuromodulators / neurotransmitters within the *Drosophila* CNS that signaling molecules often recruit specific subsets of neurons in order to produce / alter a specific behaviour. Examples include effects of OA on male social behaviour, (Certel et al., 2010) and the roles of dopamine in stress (Neckameyer and Weinstein, 2005) and of 5-HT in sleep (Yuan et al., 2008). While behaviours are controlled and coordinated centrally, the effector cells should be modulated in a manner that complements changes in motor output generated within the CNS. OA has provided evidence for a role in coordinating behaviour, from the CNS (Certel et al, 2010) to the periphery (Saraswati et al, 2003; Fox et al, 2006). Here we demonstrate independent but complementary actions of OA at the peripheral level.

Putative mechanism and model of octopamine neuromuscular modulation.

Given that co-application of the well-established tyramine receptor antagonist, yohimbine (Orchard and Lange, 1985; Saraswati et al., 2004) with OA yielded no significant departure from octopaminergic augmentation, we offer the following explanation for the independent, complimentary pre- and post-synaptic effects. Several decades of research support the hypothesis that different isoforms of OA receptors are localized pre-and post-synaptically. The original classification scheme for octopamine receptors, as suggested by Evans (1981), made a clear distinction between two main classes of OA receptors (OCTOPAMINE₁ and OCTOPAMINE₂) based mainly upon pharmacological characterizations. OCTOPAMINE₁ receptors typically yield increases in intracellular calcium, whereas OCTOPAMINE₂ is thought to mediate the activation of adenylate cyclase and subsequently modified [cAMP]_i. It is likely then, that a variant of the OCTOPAMINE₁ receptor (potentially an isoform of the OAMB receptor) is present at the presynaptic bouton. In the context of current results, it seems plausible that a member of the OCTOPAMINE₂ receptor is expressed postsynaptically. A subgroup of OCTOPAMINE_{2(B)} was stated to be located postsynaptically - on the muscle - and mediate an increase in the relaxation rate of tension (now synonymous with the β -

adrenergic-like octopamine receptors; Evans and Maqueira, 2005). Therefore, the OA-induced changes postsynaptically are potentially attributable to the activation of a second messenger system. *Drosophila* possesses many cyclic nucleotide gated channels, such as cAMP-dependent K⁺-channel, which could account for the drop in input resistance (Delgado et al, 1991; Wicher et al., 2001). Interestingly, adenylate cyclase activation typically results in cAMP-dependent phosphorylation of protein kinase A (PKA). PKA has been demonstrated to activate L-type calcium channels, which are speculated to be localized postsynaptically to larval bodywall muscle in *Drosophila* (Basavappa et al., 1999). This activation of L-type calcium channels could also be responsible for the changes in input resistance and account for an enhancement in intracellular calcium concentrations, likely yielding increased force-production.

However, our data also show a drastic increase in basal tonus, over 25 times the augmentation observed during synaptically driven contractions. An effect as prolonged as OA's effect on basal tonus could reflect changes in vital intramuscular proteins contributing to force production. Actin, myosin, and troponin / tropomyosin interactions cannot account for the prolonged, augmented state of contractibility often observed in muscle physiology (e.g. blaschko effect or catch tension; Krans, 2010). Recent evidence provides support that elastic proteins of the muscle (giant sarcomere associated proteins or gSAPs) that interact with actin / myosin may be responsible for such phenomena (Hooper and Thuma, 2005, Hooper et al., 2008, Nishikawa et al., 2012). The *Drosophila* sallimus gene encodes multiple gSAPs and the repeating PEVK domain of titin, the largest protein known and the third most abundant protein in striated muscle. If gSAP function is similar across phyla, then any number of the gSAPs may form a cross-bridge facilitating an indirect, long-lasting bond between actin and myosin resulting in the persistent effect on basal tonus observed here. It is noteworthy that PKA has previously been demonstrated to phosphorylate titin (Kruger and Linke, 2006), and that in chordate fibers, calcium influx – here putatively augmented by PKA –increases titin stiffness (Labeit et al., 2003). Thus, the putative downstream action of OA on OCTOPAMINE_{2B} receptors being a change in [cAMP] provides a pathway for physiologic modulation of the gSAPs, which is consistent with the exceptional change in

basal tonus reported here and changes in work capacity reported elsewhere (Evans and Siegler, 1982).

Abbreviations

5-HT: serotonin

Ca²⁺: calcium

cAMP: cyclic adenosine monophosphate

CNS: central nervous system

EJP: excitatory junction potential

gSAP: giant sarcomere associated protein

K⁺: potassium

NMJ: neuromuscular Junction

OA: octopamine

PKA: protein kinase A

PLTX-II: ω -plectoxin-Pt1a

PNS: peripheral nervous system

Acknowledgements and Funding

The authors would like to thank Mr. Anthony Scibelli for technical support and the recordings he made for figure 2. This work was supported by a WNE Faculty Research Grant to JLK, a Discovery Grant from NSERC to AJM; NSERC PGS and a Queen Elizabeth II Scholarship in Science and Technology to KGO.

References

- Adams, M. E. and O'Shea, M.** (1983). Peptide cotransmitter at a neuromuscular junction. *Science*. **221**, 286-9.
- Adams, M. E., Bishop, C. A. and O'Shea, M.** (1989). Functional consequences of peptide cotransmission in arthropod muscle. *Amer. Zool.* **29**, 1321-30
- Adamo, S. A., Linn, C.E., and Hoy, R.R.** (1995). The role of neurohormonal octopamine during 'fight or flight' behaviour in the field cricket *Gryllus bimaculatus*. *J. Exp. Biol.* **198**, 1691-700.
- Ahn, A.N. and Full, R.J.** (2002). A motor and a brake: two leg extensor muscles acting at the same joint manage energy differently in a running insect. *J. Exp. Biol.* **205**, 379-89.
- Basavappa, S., Mangel, A. W., Scott, L., and Liddle, R. A.** (1999). Activation of calcium channels by cAMP in STC-1 cells is dependent upon Ca^{2+} calmodulin-dependent protein kinase II. *Biochem Biophys Res Comm.* **254**, 699-702.
- Battelle, B. A. and Kravitz, E. A.** (1978). Target of octopamine action in the lobster: cyclic nucleotide changes and physiological effects in hemolymph, heart and exoskeletal muscle. *J Pharmacol Exp Ther* **205**, 438-48.
- Bier E.** (2005) *Drosophila*, the golden bug, emerges as a tool for human genetics. *Nat. Rev. Genet.* **6**, 9-23.
- Bellah, K. L. Fitch, G.K., and Kammer, A. E.** (1984). A central action of octopamine on ventilation frequency in *Corydalus cornutus*. *J. Exp Zool.* **231**, 289-92.
- Blenau, W. and Baumann, A.** (2001). Molecular and pharmacological properties of insect biogenic amine receptors: lessons from *Drosophila melanogaster* and *Apis mellifera*. *Arch. Ins. Biochem. Physiol.* **48**, 13–38.
- Blumenthal, E. M.** (2003). Regulation of chloride permeability by endogenously produced tyramine in the *Drosophila* malpighian tubule. *Am. J. Physiol. Cell. Physiol.* **284**, 718-28.
- Branton, W.D., Kolton, L., Jan, Y. N., and Jan, L. Y.** (1987). Neurotoxins from Plectreurys spider venom are potent presynaptic blockers in *Drosophila*. *J Neurosci.* **7**, 4195-200.

- Bradley, R. J., Harris, R. A., Jenner, P., Budnik, V., and Gramates, L. S.** (1999). *Neuromuscular Junctions in Drosophila: Neuromuscular Junctions in Drosophila* (Vol. 43). Academic Press.
- Clark, J., Milakovic, M., Cull, A., Klose, M. K., and Mercier, A. J.** (2008). Evidence for postsynaptic modulation of muscle contraction by a drosophila neuropeptide. *Peptides*. **29**, 1140-9.
- Certel, S. J., Leung, A., Lin, C-Y., Perez, P., Chiang, A-S., and Kravitz, E. A.** (2010). Octopamine neuromodulatory effects on a social behaviour decision-making network in *Drosophila* males. *PloS One*. **5**, e13248.
- David, J.R.** (1962). A new medium for rearing *Drosophila* in axenic condition. *Drosophila Info Serv* **36**, 128.
- del Castillo, J. and Katz, B.** (1954). Action, and spontaneous release, of acetylcholine at an inextensible nerve-muscle junction. *J. Physiol.* **126**, 27P.
- Delgado, R., Hidalgo, P., Diza, F., Latorre, R., and Labarca, P.** (1991). A cyclic AMP-activated K⁺ channel in *Drosophila* larval muscle is persistently activated in dunce. *PNAS*. **88**, 557-60.
- Downer, R.G.** (1979). Trehalose production in isolated fat body of the American cockroach, *Periplaneta Americana*. *Comp Biochem Physiol.* **62C**, 31-34.
- Evans, P.D.** (1981). Multiple receptor types for octopamine in the locust. *J Physiol.* **318**, 99-122.
- Evans, P. D. and Maqueira, B.** (2005). Insect octopamine receptors: a new classification scheme based on studies of cloned *Drosophila* G-protein coupled receptors. *Invert Neurosci.* **5**, 111-8.
- Evans, P. D. and Siegler, M. V.** (1982). Octopamine mediated relaxation of maintained and catch tension in locust skeletal muscle. *J. Physiol*, **324**, 93-112.
- Erspamer, V., and Boretti, G.** (1951). Identification and characterization by paper chromatography of enter amine, octopamine, tyramine, histamine, and allied substances in extracts of posterior salivary gland of *Octopoda* and in other tissue extracts of vertebrates and invertebrates. *Arch. Int. Pharmacodyn.* **88**, 296-332.

623 **Feng, Y., Ueda, A., Wu, C.-F.** (2004) A modified minimal hemolymph-like solution,
624 HL3.1, for physiological recordings at the neuromuscular junctions of normal and
625 mutant *Drosophila* larvae. *Neurogenetics* **18**, 377–402.

626 **Fields, P. E., and Woodring, J. P.** (1991). Octopamine mobilization of lipids and
627 carbohydrates in the house cricket, *Acheta domesticus*. *J. Insect Physiol.* **3**, 193–
628 199.

629 **Fisher, L., and Florey, E.** (1983). Modulation of synaptic transmission and excitation-
630 contraction coupling in the opener muscle of the crayfish, *Astacus leptodactylus*, by
631 5-hydroxytryptamine and octopamine. *J. Exp. Biol.* **102**, 187-98.

632 **Florey, E. and Rathmayer, M.** (1978). The effects of octopamine and other amines on
633 the heart and on neuromuscular transmission in decapod crustaceans: further
634 evidence for a role as neurohormone. *Comp. Biochem. Physiol.* **61C**, 229-237.

635 **Fox, L. E. Soll, D.R. and Wu, C.F.** (2006). Coordination and modulation of locomotion
636 pattern generators in *Drosophila* larvae: effects of altered biogenic amine levels by
637 the tyramine beta hydroxylase mutation. *J Neurosci.* **26**, 1486-98.

638 **Fritz, L. C., Wang, C. C., and Gorio, A.** (1979). Avermectin B1a irreversibly blocks
639 postsynaptic potentials at the lobster neuromuscular junction by reducing muscle
640 membrane resistance. *PNAS.* **4**, 2062-6.

641 **Grundfest, H and Reuben, J.P.** (1961). *Neuromuscular synaptic activity in lobster*. In
642 *Nervous inhibition* (ed. E. Florey), pp. 92-104. Oxford, Pergamon Press.

643 **Hidoh, O. and Fukami, J.** (1987). Presynaptic modulation by octopamine at a single
644 neuromuscular junction in the mealworm (*Tenebrio molitor*). *J. Neurobio.* **18**, 315-26.

645 **Hille, B.** (2001). *Ion channels of excitable membranes*. 3rd Ed. 814 pp. Massachusetts,
646 Sinauer Assoc. Inc.

647 **Hoang, B. and Chiba, A.** (2001). Single-cell analysis of *Drosophila* larval
648 neuromuscular synapses. *Dev Biol.* **229**, 55-70.

649 **Hooper, S. L., Hobbs, K. H., and Thuma, J. B.** (2008). Invertebrate muscles: thin and
650 thick filament structure; molecular basis of contraction and its regulation, catch and
651 asynchronous muscle. *Prog Neurobiol.* **86**, 72-127.

652 **Hooper, S., and Thuma, J. B.** (2005). Invertebrate muscles: muscle specific genes and
653 proteins. *Physiol. Rev.* **85**, 1001-60.

- Hoyle, G.** (1975). Evidence that insect dorsal unpaired median (DUM) neurons are octopaminergic. *J. Exp. Zool.* **193**, 425-31.
- Jin, L., Udo, H., Rayman, J.B. Puthanveetil, S, Kandel, E. R. and Hawkins, R. D.** (2012). Spontaneous transmitter release recruits postsynaptic mechanisms of long-term and intermediate-term facilitation in *Aplysia*. *PNAS*. **109**, 9137-42.
- Keshishian, H., Broadie, K., Chiba, A. and Bate, M.** (1996). The *Drosophila* neuromuscular junction: model system for studying synaptic development and function. *Annu. Rev. Neurosci.* **19**, 545-75.
- Klassen, L.W. and Kammer, A.E.** (1985). Octopamine enhances neuromuscular transduction in developing adult moths, *Manduca sexta*. *J. Neurobiol.* **16**, 227-43
- Krass, J. L.** (2010) The sliding filament theory of muscle contraction. *Nat. Edu.* **3**, 66.
- Kravitz, E. A., Evans, P.D., Talamo, B. R., Wallace, B. G. and Battelle, B. A.** (1976). Octopamine neurons in lobster: location, morphology, release of octopamine and possible physiological role. *CSH Symp. Quant. Biol.* **40**, 127-33.
- Kravitz, E. A., Glusman, S., Harris-Warrick, R. M., Livingstone, M. S., Schwarz, T., and Goy, M. F.** (1980). Amines and a peptide as neurohormones in lobsters: actions on neuromuscular preparations and preliminary behavioural studies. *J. Exp. Biol.* **89**, 159-75.
- Kravitz, E.A.** (1988). Hormonal control of behavior: amines and the biasing of behavioral output in lobsters. *Science*. **30**, 1775-81.
- Kruger, M., and Linke, W. A.** (2006). Protein kinase-A phosphorylates titin in human heart muscle and reduces myofibrillar passive tension. *J. Musc. Res. Cell Motil.* **27**, 435-44.
- Labeit, D., Watanabe, K., Witt, C., Fujita, H., Wu, Y., Lahmers, S., Funck, T., Labeit, S. and Granzier, H.** (2003) Calcium-dependent molecular spring elements in the giant protein titin. *PNAS* **100**, 13716–13721.
- Leung H.-T., Branton, W. D., Phillips, H. S., Jan L, and Byerly, J.** (1989) Spider toxins selectively block calcium currents in *Drosophila*. *Neuron* **3**, 767-772.
- Lnenicka, G. A. and Mellon, D. Jr.** (1983). Changes in electrical properties and quantal current during growth of identified fibers in the crayfish. *J. Physiol.* **345**, 261-84.

685 **Macleod, G.T., Hegstrom-Wojtowicz, M., Charlton, W.P., Atwood, H.L.,** (2002). Fast
686 calcium signals in *Drosophila* motor neuron terminals. *J. Neurophys.* **88**, 2659–2663.

687 **Martin, A.R.** (1976). The effect of membrane capacitance on non-linear summation of
688 synaptic potentials. *J. Theor. Biol.* **59**, 179–187.

689 **McLachlan, E.M., Martin, A.R.** (1981). Non-linear summation of end-plate potentials in
690 the frog and mouse. *J. Physiol.* **311**, 307–324.

691 **Meyrand, P. and Marder, E.** (1991). Matching neural and muscle oscillators: control by
692 FMRFamide-like peptides. *J. Neurosci.* **11**, 1150-61.

693 **Monastirioti, M., Gorczyca, M., Rapus, J., Eckert, M., White, K., and Budnik, V.**
694 (1995). Octopamine immunoreactivity in the fruit fly *Drosophila melanogaster*. *J.*
695 *Comp. Neurol.* **356**, 275-87.

696 **Nagaya, Y., Kutsukake, M., Chiquisa, S. I., and Komatsu, A.** (2002). A trace amine,
697 tyramine, functions as a neuromodulator in *Drosophila melanogaster*. *Neurosci Let.*
698 **329**, 324-8.

699 **Neckameyer, W. S. and Weinstein, J. S.** (2005). Stress affects dopaminergic signaling
700 pathways in *Drosophila melanogaster*. *Stress.* **8**, 117-31.

701 **Nishikawa, K. C., and Monroy, J. A., Uyeno, T. E., Yeo, S. H. Pai, D. K., and**
702 **Lindstedt, S. L.** (2011). Is titin a ‘winding’ filament? A new twist on muscle
703 contraction. *Proc. R. Soc. B.* **279**, 981-90.

704 **O’Gara, B. and Dewes, C. D.** (1990). Modulation of tension production by octopamine
705 in the metathoracic dorsal longitudinal muscle of the cricket *teleogryllus oceanius*. *J.*
706 *Exp. Biol.* **149**, 161-76.

707 **O’Shea, M., and Evans, P. D.** (1979). Potentiation of neuromuscular transmission by
708 an octopaminergic neurone in the locust. *J. Exp. Biol.* **79**, 169-90.

709 **Orchard, I., Carlisle, J. A., Loughton, B. G., Gole, J. W. and Downer, R. G.** (1982).
710 *In vitro* studies on the effects of octopamine on locust fat body. *Gen. Comp.*
711 *Endocrin.* **48**, 7-13.

712 **Orchard, I. and Lange, A. B.** (1985). Pharmacological profile of octopamine receptors
713 on the lateral oviducts of the locust, *Locusta migratoria*. *J. Insect Physiol.* **32**, 741-
714 45.

- Ormerod, K. G., Hadden, J. K., Scibelli A., Milakovic, M., Mercier, A. J., and Krans, J. L.** (2012) Octopamine and tyramine modulate synaptic properties and muscle contractions in *Drosophila*. 887.12 Neuroscience Meeting Planner. New Orleans, LA: Society for Neuroscience
- Paterson, B. A., Anikin, I. M., and Krans, J. L.** (2010). Hysteresis in the production of force by larval Dipteran muscle. *J. Exp Biol.* **213**, 2483-93.
- Peron, S., Zordon, M. A., Magnabosco, A., Reggiani, C., and Megighian, A.** (2009). From action potential to contraction: Neural control of excitation-contraction coupling in larval muscles of *Drosophila*. *Comp. Biochem. Physiol.* **154**, 173-83.
- Pfluger, H.-J., and Stevenson, P. A.** (2005). Evolutionary aspects of octopaminergic systems with emphasis on arthropods. *Arthr. Struct. Dev.* **34**, 379-96
- Quigley, P.A. and Mercier, A.J.** (1997). Modulation of crayfish superficial extensor muscle by a FMRFamide-related neuropeptide. *Comp. Biochem Physiol.* **118A**, 1313-20.
- Rane, S. G., Gerlach, P. H., and Wyse, G. A.** (1984). Neuromuscular modulation in Limulus by both octopamine and proctolin. *J. Neurobiol.* **15**, 207-20.
- Roeder, T.** (1999). Octopamine in invertebrates. *Prog. Neurobiol.* **59**, 533-61.
- Roeder, T.** (2005). Tyramine and octopamine: Ruling behavior and metabolism. *Ann. Rev. Entomol.* **50**, 447-77.
- Saraswati, S., Fox, L.E., Soll, D.R., and Wu, C.F.** (2004). Tyramine and octopamine have opposite effects on the locomotion of *Drosophila* larvae. *J Neurobiol.* **58**, 425-41.
- Stevens, C.F.** (1976). A comment on Martin's relation. *Biophysic J* **16**, 891–895.
- Stewart, B. A., Atwood, H. L., Renger, J. J., Wang, J. and Wu, C.-F.** (1994). Improved stability of *Drosophila* larval neuromuscular preparations in haemolymph like physiological solutions. *J. Comp. Physiol. A* **175**, 179-191.
- Velez, S.J. and Wyman, R.J.** (1978). Synaptic connectivity in a crayfish neuromuscular system. II. Nerve-muscle matching and nerve branching patterns. *J Neurophysiol.* **41**, 85-96.
- Verlindin, H., Vleugels, R., Marchal, E., Badisco, L., Tobback, J., Pfluger, H-J., Blenau, W., and Broeck, J. V.** (2010). The cloning, phylogenetic relationship and

distribution patter of two putative GPCR-type octopamine receptors in the desert locust. *J. Insect Physiol.* **56**, 868-75.

Walther, C. and Zittlau, K. E. (1998). Resting membrane properties of locust muscle and their modulation II. Actions of the biogenic amine octopamine. *J. Neurophys.* **80**, 785-97.

Wheal, H. V. and Kerkut, G. A. (1976). The pre- and post-synaptic actions of 5-HT in crustacean. *Comp. Biochem. Physiol* **54C**, 67-70.

Whim, M. D., and Evans, P. D. (1988). Octopaminergic modulation of flight muscle in the locust. *J Exp Biol* **134**, 247-266

Whim, M.D., and Evans, P. D. (1989). Age-dependence of octopaminergic modulation of flight muscle in the locust. *J. Comp. Physiol. [A]* **165**, 125-37.

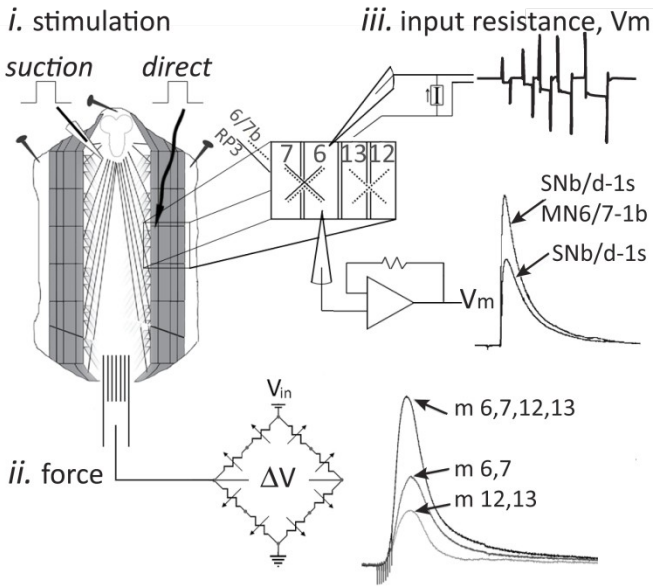
Wicher, D., Walther, C., and Wicher, C. (2001). Non-synaptic ion channels in insects – basic properties of currents and their modulation in neurons and skeletal muscles. *Prog. Neurobiol.* **64**, 431-525.

Wierenga, J.M and Hollingworth, R.M. (1990). Octopmaine uptake and metabolism in the insect nervous system. *J. Neurochem.* **54**, 479-89.

Yuan, Q., Joiner, W. J., and Sehgal, A. (2008). A sleep-promoting role for the *Drosophila* serotonin receptor 1A. *Curr Biol.* **16**, 1051-62.

Zill, S. N., Moran, D.T., and Varela, F.G. (1981). The exoskeleton and insect proprioception. II. Reflex effects of tibial campaniform sensilla in the American cockroach, *Periplaneta Americana*. *J Exp Bio.* **94**, 43-55.

A EVOKED CONTRACTIONS



B BASAL TONUS

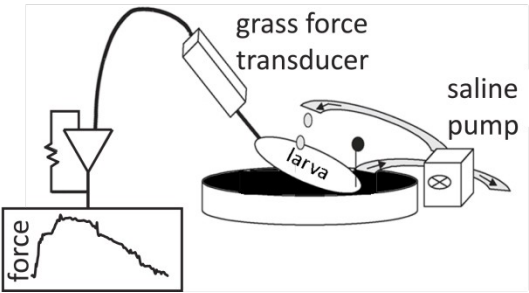
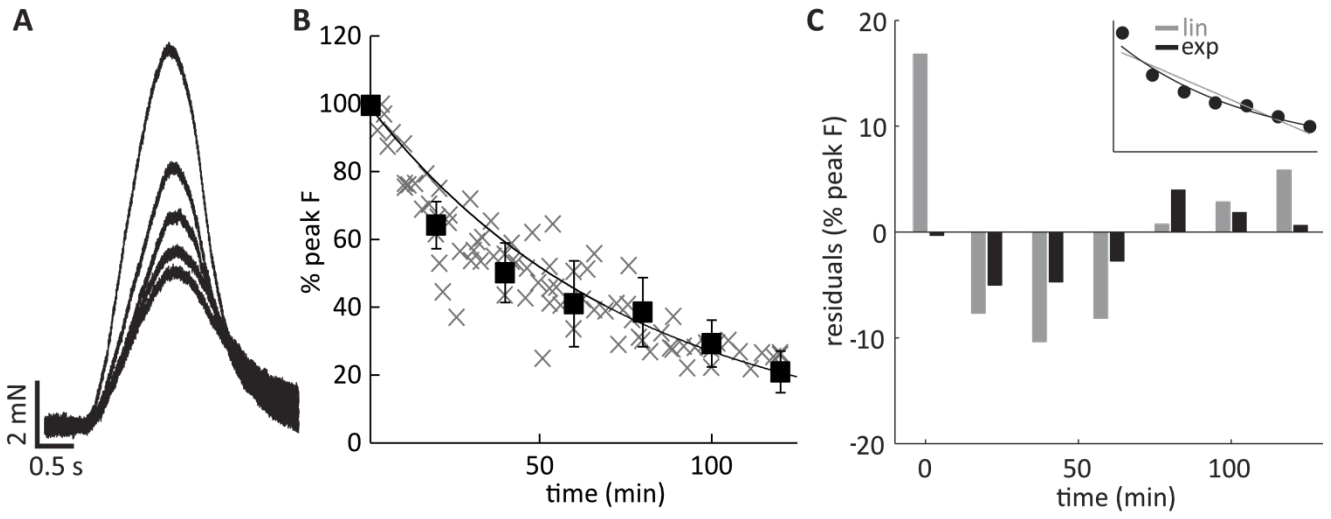
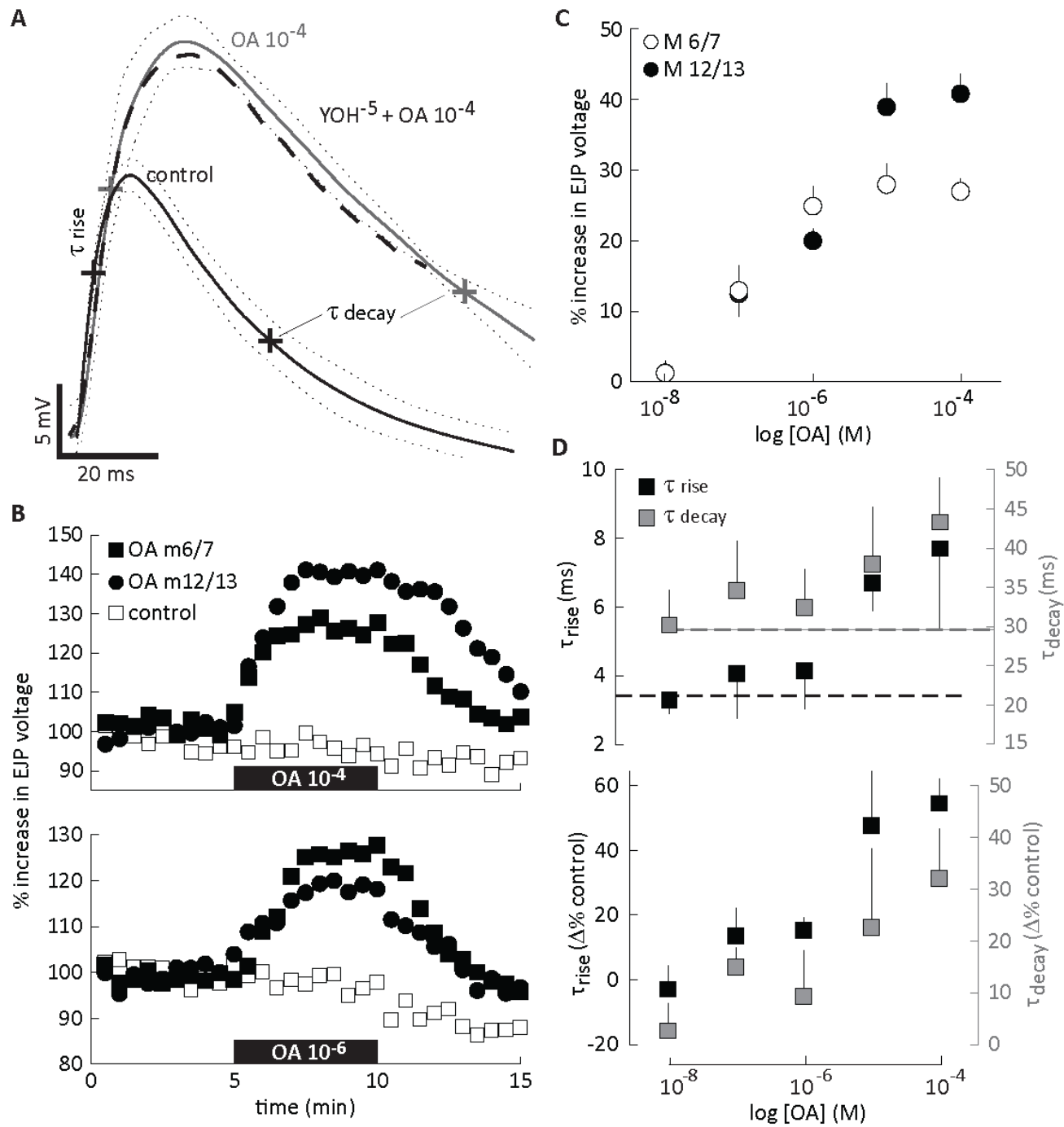
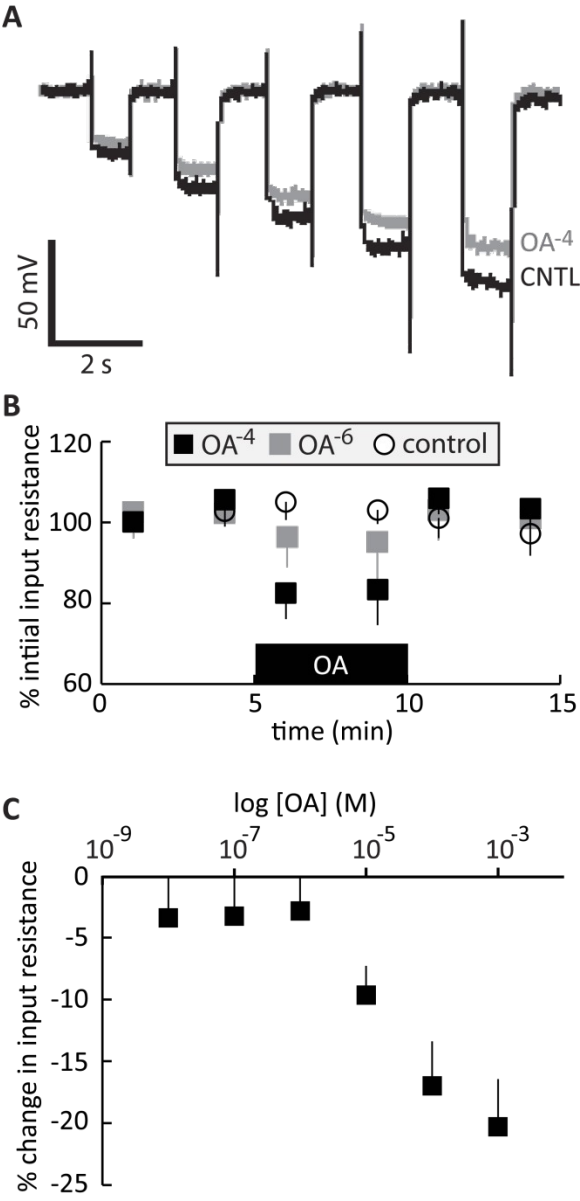


FIGURE 2





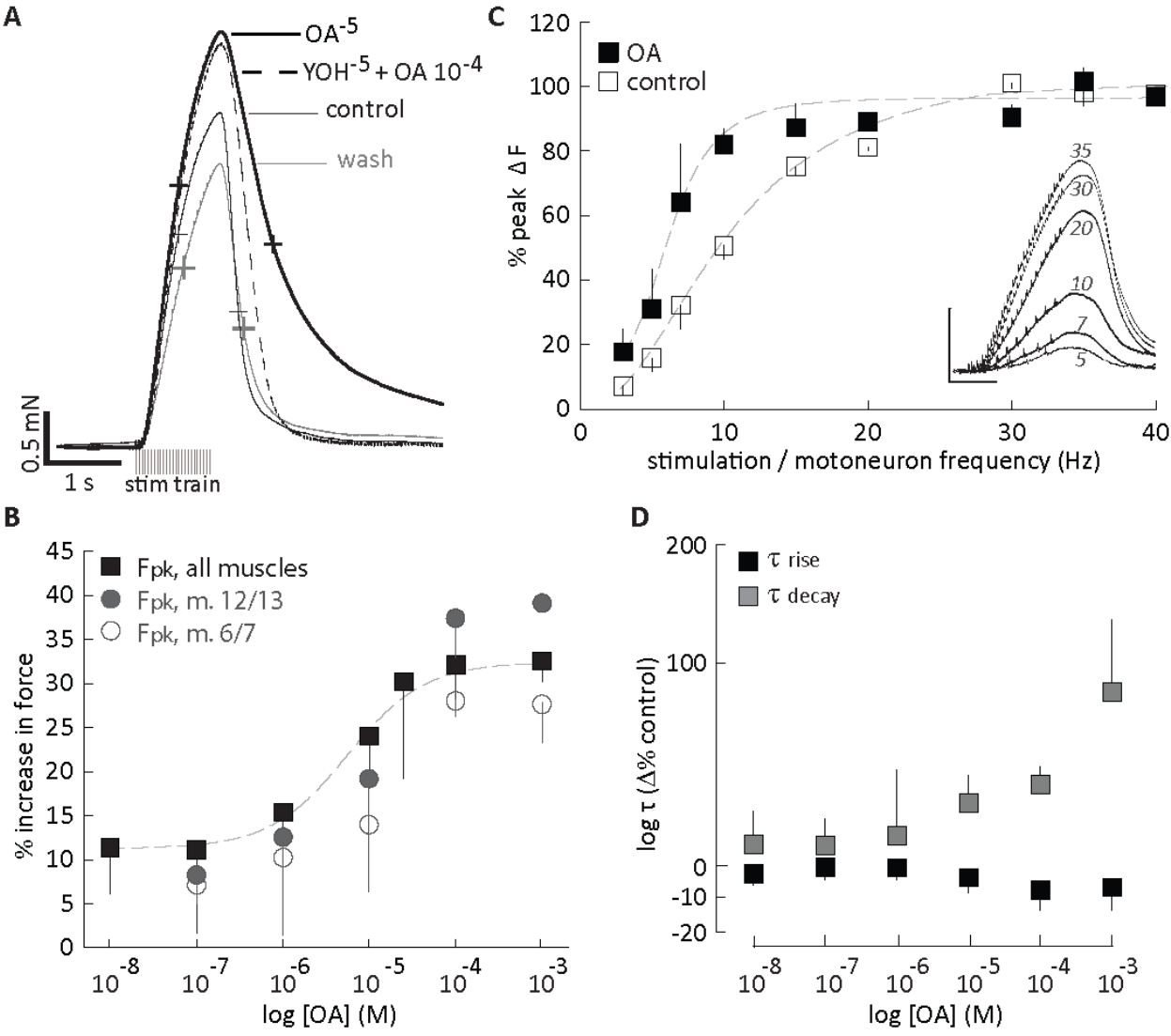
781 **FIGURE 4**

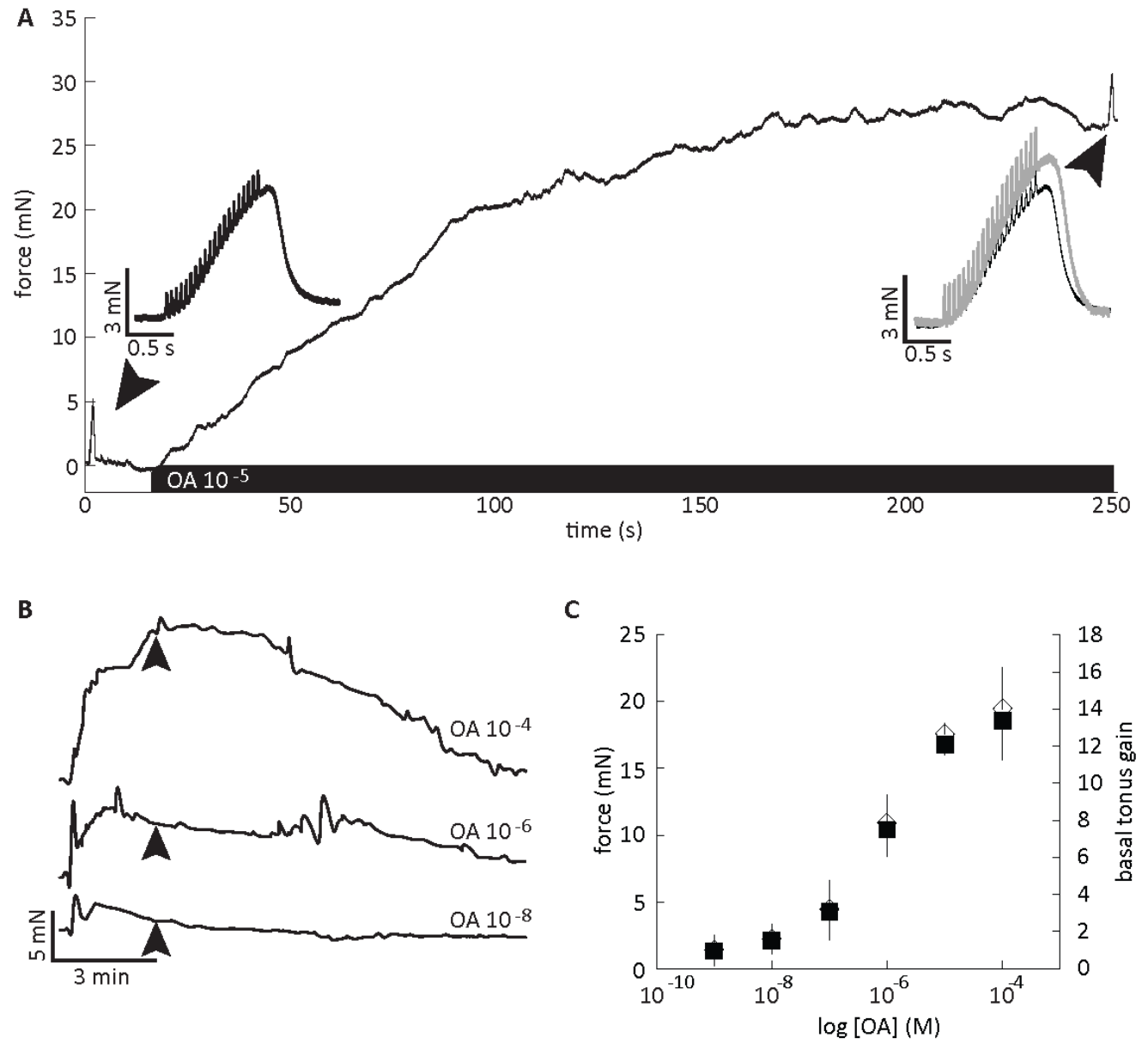


782

783

784 **FIGURE 5**



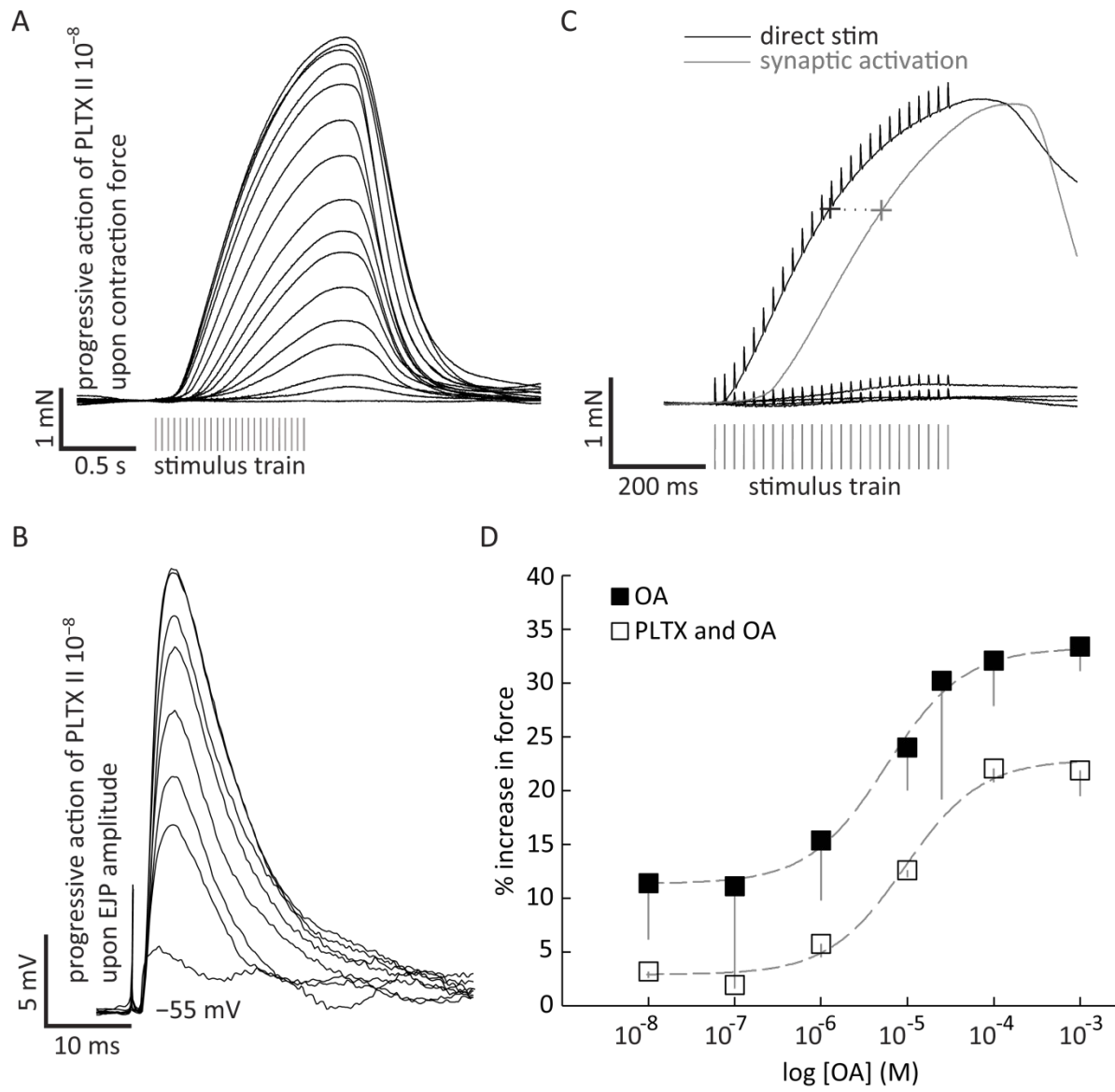


790

791

792

793



795

796

797

Legends

Figure 1. Semi-intact preparation used for recording force and intracellular electrical signals. **A.** The schematic of a filleted larva highlights larval bodywall longitudinal muscles (m 6, 7, 12 and 13), which produced the gross majority of longitudinal force discussed herein. Transverse muscles are indicated by fading light gray, outlined in the center of the schematic. **i.** Segmental nerves are shown as black lines radiating from the ventral ganglion (top). Both stimulating techniques, suction electrode and direct stimulating electrode, are indicated. **ii.** A hook placed upon the posterior portion of the preparation connects the beam of the force transducer, which utilizes a custom double bridge orientation of silicon wafers. **iii.** An amplifier was used to inject current and record voltage from a single intracellular electrode. Muscle fibers were either injected with a series of currents (4, 6, 8, 10, 12 pA) and the voltage responses were recorded, or membrane potential was recorded passively concurrent with suction stimulation to presynaptic nerves. **B.** Basal tonus was recorded using an established method (see text) and an FTO3 Grass tension transducer and amplifier. The CNS was eviscerated and saline, with or without octopamine, was washed over the preparation.

Figure 2: Time dependent decrease in contraction amplitude. **A.** Contraction force decreases with time, more notably in the first 30 minutes of recording then thereafter (times after initial recording are given). **B.** Inasmuch, an exponential function ($F_{pk} = e^{-0.013 * t}$) provides a statistically significant fit of the decay in contraction amplitude ($R^2 = 0.95$, $P < 0.01$, Pearson's Correlation, $n = 10$). Gray x's are individual F_{pk} data from all 10 animals, solid squares are mean F_{pk} values across all 10 animals. **C.** Residuals from both linear (gray: $F_{pk} = -0.0076t + 1$; $\bar{x} = 7.48$) and exponential functions (black: $\bar{x} = 2.74$) were examined to identify the simplest function that reasonably fit the decay in contraction amplitude.

Figure 3: Octopamine augmentation of Excitatory Junction Potentials (EJPs). **A.** Averaged EJP waveforms in control saline (black), and octopamine-containing saline

(gray) are plotted with their respective 95% confidence intervals (dots, n=5 each). Co-application of yohimbine (10^{-5} M) with 10^{-4} M [OA] falls within the confidence interval of OA alone (dashed line). Points at which rise and decay time constants were computed are marked; ~63% of peak and decay voltage, each. **B.** EJP amplitude is plotted over 15 minutes to demonstrate the rate of reversibility / washout at two doses. Horizontal black bars indicate when OA is applied. **Top** above 10^{-4} M [OA], washout required two times the exposure duration, whereas below 10^{-5} M (**bottom**), reversibility begins immediately upon washout. **C.** EJP amplitude increased with [OA] in a dose-dependent manner. The action upon m 12/13 was greater than m 6/7 at high doses. **D. Top** Both rise and decay time constants increased with [OA] (n=5, each point). Time constants of control traces (τ_{rise} : black dashed; τ_{decay} : gray dashed) are plotted (n=25 each). **Bottom** Changes in time constants are plotted as percent of control values.

Figure 4: **Total membrane resistance changes as a function of [OA]. A.** A series of hyperpolarizing current pulses was passed (4, 6, 8, 10, and 12 pA) and the resultant voltages from muscles 6, 7, 12, or 13 were recorded. Pulse duration was increased with current amplitude to estimate asymptotes of voltage deflections. **B.** Two time series of data are given to demonstrate the immediate reversibility of changes in total membrane resistance at even high concentrations of OA (i.e. 10^{-4} M). **C.** Total membrane resistance was statistically different than control at and above 10^{-5} M [OA] ($P < 0.01$, each compared to control).

Figure 5: **Action of octopamine on synaptically driven force production. A.** Averaged contractions (n=8-10 repetitions, each) driven by 25 Hz stimulation of the motor nerve for one second: prior to application of OA (black: control), during bath application of OA-containing saline (thick black: [OA] 10^{-5} M), co-application of yohimbine (10^{-5} M) with 10^{-4} M [OA] (dashed line), and upon washout (gray: wash). Crosshairs indicate the points used to compute time constants (τ , latency from preceding force inflection: either onset of contraction or relaxation). **B.** OA-dependent augmentation of contraction; dose-response curve. The OA dependence of peak force (F_{pk}) from synaptically evoked contractions (n=33 total). The response of all four muscle

fibers is shown in black squares (n=33). Open circles indicate that muscles 12 and 13 were ablated while m. 6 and 7 were left intact (n=11). In contrast, filled circles indicate that m. 12 and 13 were intact whilst m 6. and 7. were ablated (n=12). **C.** Force-frequency curve for OA and control groups. The force-frequency (motoneuron) relationship shifts left in OA-containing saline ($5.5 \cdot 10^{-6}$ M [OA] selected from the dose response curve above; EC_{50}) Inset: Muscle contraction (raw recordings) at varying frequencies. **D.** Time constants of contraction change with [OA] in a manner consistent with increased contraction duration (n=31 preparations). τ_{rise} decreases, reaching peak force in less time, while τ_{decay} increases, maintaining force longer (see text). Standard deviation plotted in panel **D**.

Figure 6: Action of octopamine on basal tonus. **A.** Force was recorded whilst stimuli were delivered to the segmental nerves at 25 Hz (duration = 1 s) immediately prior to application of OA (inset left: black), and about four minutes later (inset right: gray; again 25 Hz for 1 s), at the peak of octopamine's action on basal tonus. **B.** With the segmental nerves severed and CNS removed, five minutes of octopamine application augmented basal tonus. The amplitude of augmentation was measured three minutes (black arrows) post-application. **C.** OA increased basal tonus in a dose-dependent manner in preparations lacking electrical stimulation. Contraction data represent mean force and gain (ratio of tonus prior to application and during application of OA).

Figure 7: Directly activated contractions are also augmented by octopamine. **A.** Upon application of PLTX, contraction amplitude (not averaged) decreases with time; each trace reflects a two minute interval. Stimuli are delivered to the segmental nerve / motoneurons at 25 Hz for 1 s. **B.** EJPs (not averaged) recorded from the longitudinal muscles demonstrate the progressive failure of the synapse; each trace reflects a 40 s interval. **C.** Contraction traces (not averaged) before and after 30 minutes exposure to PLTX. Lines with stimulus artifact were collected upon direct stimulation / depolarization (black). The contraction immediately preceding application of PLTX is shown in gray (no artifacts). Points at which rise time constants were measured are marked on each contraction trace. The stimulus trains (identical) used to evoke each

891 contraction are shown in gray beneath the contractions. **D.** OA augmentation of
892 contraction amplitude when evoked synaptically (filled squares; re-plotted from Figure
893 5) or via direct stimulation of the muscle in PLTX (open squares, n=22).

894

895